An Anthropomorphic Robotic Hand with a Soft-Rigid Hybrid Structure and Positive-Negative Pneumatic Actuation

Chaozhou Zhang, Min Li, *Member, IEEE*, Yushen Chen, Zhanshuo Yang, Bo He, Xiaoling Li, Jun Xie, and Guanghua Xu, *Member, IEEE*

***Abstract*—Anthropomorphic robotic hands are seeking to achieve key features such as multi-degree-of-freedom motion ability, bi-directional actuation, high adaptability, and sufficient stiffness. In this research, we propose a 10 active degrees-of-freedom anthropomorphic robotic hand with a soft-rigid hybrid structure and positive-negative pneumatic actuation. The fingers of the hand utilize pneumatic actuators composed of soft bellows to actuate a rigid skeleton for bending motion with unidirectional-stretchable nylon elastic fabric as a strain limiting layer. The positive-negative pneumatic actuation mimics the flexors and extensors of the human hand to implement bi-directional finger actuation. We present a prototype implementation of this robotic hand and provide a preliminary evaluation. The experimental results show that the combined positive-negative pneumatic actuation can extend the workspace of the finger and increase the finger stiffness compared to using only positive pneumatic actuation. The proposed robotic hand has good comprehensive performance (generated a blocking force of 7.5 N, scored 7 in the Kapandji test, achieved 32 of the 33 grasp postures from the Feix taxonomy, and could implement 5 human grasping strategies) compared to other robotic hands in literatures.**

***Index Terms*—Anthropomorphic hand, rigid-flexible combined, soft robotics, dexterous hand**

I. Introduction

As an important part of human-computer interaction, teleoperation technology enables humans to overcome the barriers of environment and distance [1]. To a large extent, the capabilities of the robot end-effectors determine the functionality of the teleoperation system [2]. Tasks requiring interaction with humans, complex environments, or objects with complex shapes and varying hardness pose challenges to the dexterity, adaptability, and interaction safety of the end-effectors of the teleoperated robots [3].

Manuscript received December 19, 2022; Revised March 9, 2023; Accepted May 6, 2023. This paper was recommended for publication by Liu, Hong upon evaluation of the Associate Editor and Reviewers' comments. This work was supported in part by the National Natural Science Foundation of China under Grant (51975451). (*Corresponding author: Min Li*)

C. Zhang, M. Li, Y. Chen, Z. Yang, B. He, X. Li, J. Xie, and G. Xu are with the School of Mechanical Engineering, Xi'an Jiaotong University, Xi'an 710049, China. (e-mail: jixiezcz@stu.xjtu.edu.cn; min.li@mail.xjtu.edu.cn; cys105@stu.xjtu.edu.cn; YangZhuo@stu.xjtu.edu.cn; xajthx@stu.xjtu.edu.cn; xjtulxl@mail.xjtu.edu.cn; xiejun@mail.xjtu.edu.cn; xugh@mail.xjtu.edu.cn)

Digital Object Identifier (DOI): see top of this page.

The human hand has superior gripping properties because of its mixed skeletal and muscular structure, and the dexterity of its tendons [4]. Anthropomorphic multi-fingered dexterous hands, that usually have more than three fingers imitating human hand movements with higher dexterity compared with conventional mechanical grippers, conform to people's operating habits and are suitable for handling tools like a human [5]. Therefore, it has attracted wide academic attention. The design of a multi-fingered dexterous hand should not only simply pursue the imitation of human hand shape, but also be guided by in-depth analysis of the physiological structure and transmission principles of the human hand.

Anthropomorphic hands developed in the early years mostly had rigid structures that achieved movement through connecting rods driven by motors, which have the advantages of accurate force and position control [5], [6]. However, owing to the high stiffness and large output force of those rigid hands, there is a risk of damaging the object or the hand itself while performing a grasping task. Since the rigid hands lack adaptability, researchers have tried to use sensors and designed control algorithms to enable the rigid hands to grasp small, soft objects, which greatly increased the control difficulty of the system [7].

To solve these problems, soft hands, which rely on their flexibility and compliance to envelope grasping objects, have become the research hotspot in recent years. Compared to rigid hands, soft hands are more lightweight, safer to interact with, and better at gripping unstructured objects [4], [8]. Researchers often imitate the actuation modes of human tendons by using tendon antagonistic driven powered by motors to achieve joint rotation [7], [9]. However, each finger of such hands usually has only one actuated degree-of-freedom (DOF), and increasing the DOFs tends to make the structural design more difficult and increase the number of motors. In addition, due to the friction loss of the tendon routing, the life and transmission efficiency are reduced. Another commonly used type of soft hands is fluid-driven ones made from hyper-elastic materials such as silicone and flexible polymers [8], [10]. Because of the key features including fast response, streamlined structure and high power/weight ratio, there is a lot of research on robot hands with pneumatic actuators [11]. Fiber-reinforced bending actuators have been developed and fabricated through the fiber winding method to reduce non-functional deformation of the pneumatic actuators and thus to increase the output force [12],

[13]. However, that may complicate the fabrication process and make the assembly of the actuators more difficult. Polygerinos et al. attempted to design the rehabilitation glove utilizing cloth as a restraint on deformation [14]. To the best of our knowledge, simpler methods to make strain limiting layers applied on pneumatic actuators in anthropomorphic multi-fingered dexterous hands have not been reported.

In order to make the manipulator not only flexible but also with sufficient stiffness and output force, researchers have combined rigid structures and flexible materials in robotic hand designs [15], [16]. For example, Hashemi et al. [15] embedded rigid structures into a fiber-reinforced bending soft robotic finger and Zhang et al. [16] designed a soft finger that has a bioinspired hybrid structure integrating a pneumatic bellows chamber and joint skeletons. Nevertheless, the extension motion of most soft pneumatic hands, including the above-mentioned robotic hands with rigid-soft hybrid structures, relies on the resilience of the material or structure itself, even though the bi-directional actuation, namely finger flexion and extension, is critical to the robot's ability to perform the task. Some studies have realized the bi-directional actuation by using spring steel straps [17], [18]. However, normally the finger is designed with one DOF driven by one motor, limiting its use in dexterous hands. Moreover, due to gravity and the acceleration resulting from rapid movement, the initial shape of the soft pneumatic hand becomes uncontrollable. However, controlling the contact between the robotic hand and the object is important in dexterous hand grasp planning [19]. It is necessary to increase the stiffness of the soft hand before performing the grasping motion, namely the initial stiffness. Some studies have employed negative pressure to induce jamming as a means of regulating stiffness [20]. In conclusion, anthropomorphic hands are still seeking to achieve key features such as multi-DOF motion ability, bi-directional actuation, high adaptability, and enough stiffness.

In this paper, we propose a novel anthropomorphic dexterous hand with a soft-rigid hybrid structure and positive-negative pneumatic actuation. The fingers in the hand utilize pneumatic actuators composed of soft bellows to actuate a rigid skeleton for bending motion with a unidirectional-stretchable nylon elastic fabric as a strain limiting layer. The proposed robotic hand has five fingers and an arch-shaped palm. The positive-negative pneumatic actuation mimics the flexors and extensors of the human finger to implement bi-directional finger actuation. Experimental characterization and grasping experiments are presented to show the feasibility of the proposed hand.

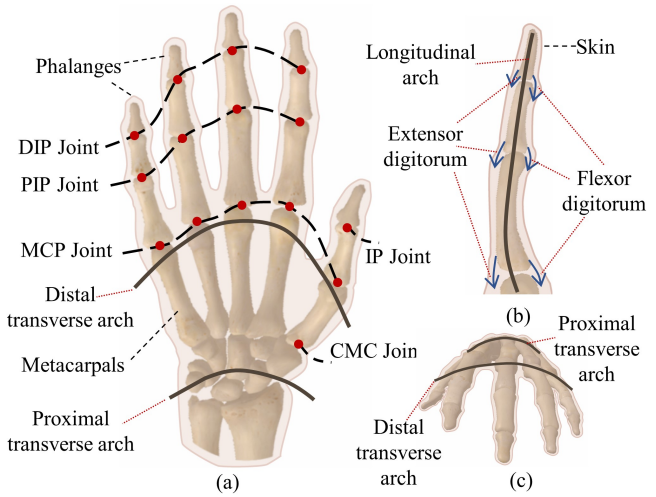

Fig. 1. Schematic of the physiological structure of human hand: (a) front view, (b) side view and (c) top view.

The main contributions of this paper are summarized as follows: (1) A method of bi-directional finger actuation achieved by positive-negative pneumatic actuation mimicking the flexors and extensors of the human hand is applied to the soft robotic hand, which expands the range of motion (ROM), reduces the time required to complete a grasping motion, and increases the initial stiffness; (2) A 10 active DOFs, simple-to-make soft-rigid hybrid anthropomorphic dexterous hand is developed, which has high-performance in output force, dexterity and other comprehensive properties; (3) A unidirectional-stretchable nylon elastic fabric is used as a strain limiting layer in a robot hand, which enlarges the bending range and improves the actuation efficiency of the pneumatic actuators, and at the same time, the assembly is much simpler than the commonly used fiber winding method.

II. Design and Fabriction

A. Human Hand Analysis

The design of the anthropomorphic robotic hand is guided by the analysis of the physiological structure and functions of human hands. The skeletal is composed of metacarpals and phalanges. The thumb has three joints, including an interphalangeal (IP) joint, a metacarpophalangeal (MCP) joint, and a carpometacarpal (CMC) joint. The remaining four fingers consist of a distal interphalangeal (DIP) joint, a proximal interphalangeal (PIP) joint, and an MCP joint (see Fig. 1 (a)). In total, the human hand has 15 joints and 21 DOFs. It is owing to the large number of joints and DOFs that human hand can perform dexterous motions. However, implementing all DOFs and full actuation in the robotic hand design would greatly increase the complexity and difficulty of control, so it is necessary to reduce the number of actuated DOFs. Extensive research has shown a strong link between the movements of the DIP and PIP joints [21]. In other words, when the PIP joint flexes, the DIP joint flexes as well with a proportional bending angle to the PIP joint. Therefore, the robotic finger can be designed as an underactuated form where DIP and PIP joints share one DOF. Owing to the complex anatomy and movements of the thumb, there has been a great deal of controversy regarding the CMC and MCP movements [22]. In our study, the movements of the thumb are considered as a combination of flexion/extension and abduction/adduction movements.

Human hands rely on the flexion and extension movements of hand arches, including transverse arches and longitudinal arches, to achieve various grasping and pinching movements. As shown in Fig. 1(a) and (c), the distal transverse arch consists of five metacarpal bones that are angled towards each

This article has been accepted for publication in IEEE Robotics and Automation Letters. This is the author's version which has not been fully edited and content may change prior to final publication. Citation information: DOI 10.1109/LRA.2023.3280829

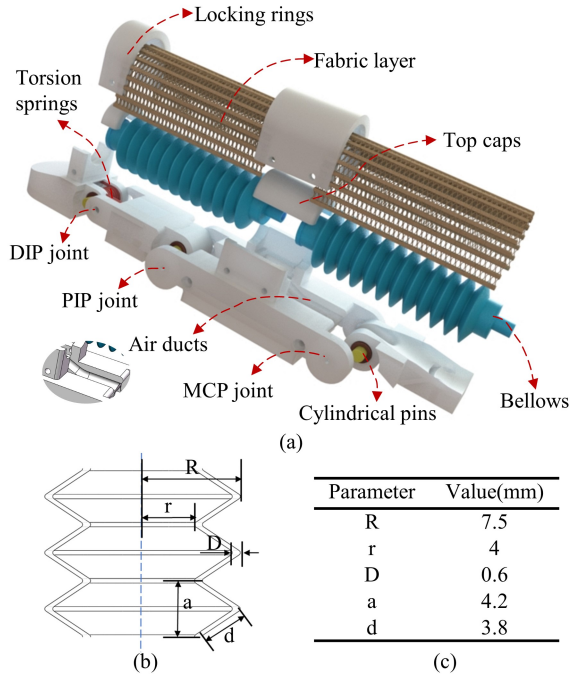

Parameter	Value(mm)
R	7.5
r	4
D	0.6
a	4.2
d	3.8

(c)

Fig. 2. Design of the soft-rigid hybrid bionic finger.

other to create a concave curvature in the palm. As shown in Fig.1(b), the longitudinal arch is composed of the metacarpophalangeal joint and articulating phalanges. There are five rows of longitudinal arches. The flexion and extension of the fingers are completed by the flexors and extensors.

Hume et al. [23] examined the hand functional ROMs for various activities of daily life (ADLs) and found that thumb was ranging from 21° to 65° and the other four fingers were ranging from 96° to 208°. The maximum extension angle for the thumb and the other four fingers is 10° and 45°, respectively [24]. According to Morales et al. [25], common objects to be grasped in ADLs weigh less than 1.50 kg.

B. Soft-Rigid Hybrid Bionic Finger Design

Based on the above human hand analysis, we propose an anthropomorphic finger design with a rigid-flexible hybrid structure (see Fig. 2(a)). This finger uses soft bellows to actuate a rigid skeleton to achieve joint rotation. Similar to human hands, the robotic finger has three joints. The rotating joints of the rigid structure are hinged through cylindrical pins and copper bushings. The DIP joint and PIP joint are linked together with a stainless-steel torsion spring (wire diameter is 1.2 mm; outer diameter is 5 mm; effective number of coils is 6; and spring angle is 180°). The ends of the soft bellows are secured to the rigid structure on either side of the rotating joints using top caps. Considering that the length of the human MCP joint is only slightly smaller than the sum length of the PIP and DIP joints [26], two off-the-shelf bellows with the same parameters are used to actuate the three joints of one finger to simplify the fabrication process (see Fig. 2(b) - (c)). The air tube connected to the PIP actuator is arranged inside the proximal phalanx (the air ducts marked in Fig. 2 (a)).

The pneumatic actuator is wrapped with a layer of unidirectional-stretchable nylon elastic fabric (a fish-mesh structure, 1 mm thickness, 40 mm width, tensile strength of 53 N/mm^2, elongation at break of 220%, and the elastic recovery of 93.8% after 1600 repeated stretches) as the strain limiting layer, which is secured to the finger by locking rings and self-locking plastic nylon cable zips. This design is mainly aimed at restraining the lateral deformation of the actuator, enlarging the bending angles, and improving energy utilization. At the same time, the fabric layer acts as the skin of the human hand, protecting the bellows and providing a restoring force when positive pressure of the actuator is unloaded.

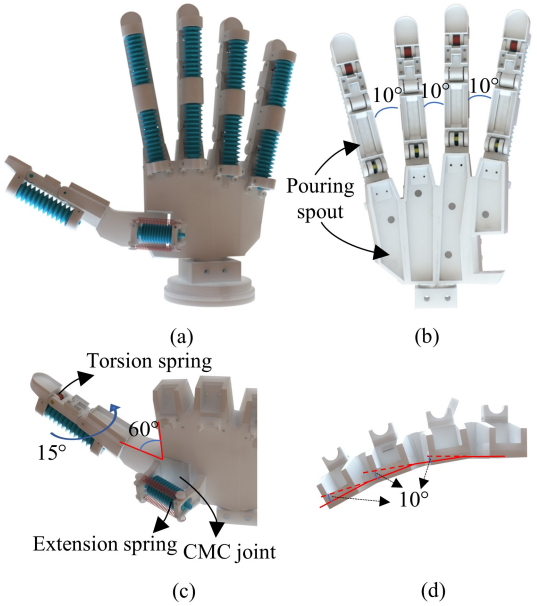

Fig. 3. Schematic diagram of the anthropomorphic hand (without fabric strain limiting layers): (a) assembly of the hand, (b) the palm side, (c) the design parameters of the thumb, and (d) the design parameters for the transverse arch of the hand.

The bellows are in a slightly contracted state when there is no air pressure added. The elastic force of the bellows is in balance with the tension of the elastic fabric layer, keeping the finger in a stable state when it is not actuated. When the bellows are filled with positive pressure, the bellows are expanded and elongated. Under the restriction of the rotation of the rigid structure, the upper and lower sides of the bellows are asymmetrically elongated to actuate the fingers and complete the flexion movement. Similarly, when the bellows are charged with negative pressure, the bellows contract to actuate the finger to accomplish an extension motion.

C. Anthropomorphic Dexterous Hand Design and Integration

Fig. 3 shows the design schematic of the anthropomorphic robotic hand. The hand consists of four similarly constructed fingers, a thumb module, and an arch-shaped palm, with a total of 15 DOFs and 10 degrees of actuation.

As shown in Fig. 3(c), the thumb module has three joints including CMC, MCP, and IP. The thumb is designed with two DOFs that allow for flexion/extension and abduction/adduction movements. The elongation of fabric layer utilized in this study is not suitable for the CMC joint. Instead, two tension springs are used to provide recovery force for the bellow and help CMC joint remain stable when the thumb is not actuated. To simulate the transverse arch of the

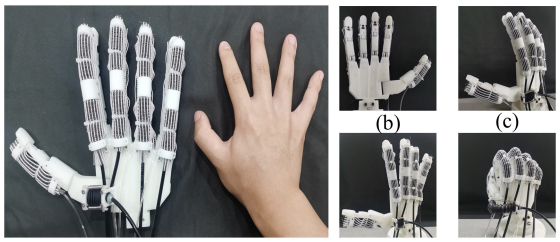

Fig. 4. The prototype of the proposed robotic hand: (a) the hand size compared with a human hand, (b) the palm side, (c) the relaxing state with no actuation, (d) the extension state with negative actuation, and (e) the flexion state with positive actuation.

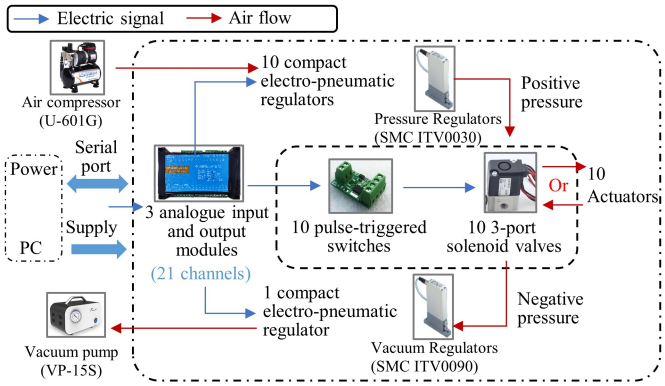

Fig. 5. Control flow chart of the robotic hand.

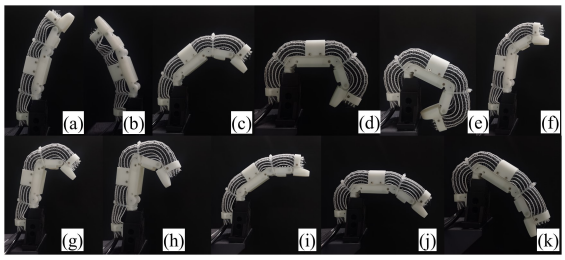

Fig. 6. The index finger postures: (a) at a relaxing state without actuation, (b) with extension actuation, (c)-(e) when the two actuators are actuated simultaneously, and (f)-(h) and (i)-(k) when the two actuators are actuated separately with positive pressures.

human hand, each two adjacent metacarpal bones form an angle of 10° (see Fig. 3(d)).

Fig. 4 shows the prototype of the anthropomorphic dexterous hand. All rigid skeleton structures of the fingers and palms are 3D-printed using PLA material. Air tubes with a diameter of 2 mm and 4 mm are used to connect the PIP and MCP actuators, respectively. The connecting areas are sealed with sealing tape and silicone sealant (RTV108, Momentive Performance Materials, USA) to ensure airtightness. A layer of silicone rubber (Dragon Skin 10 Medium, Smooth-On, USA) was casted on the surface of the fingertips and palms to increase grip friction (see Fig. 3(b)).

D. Positive-Negative Pneumatic Actuation and Control

To realize the independent 10 active DOFs actuation of the robotic hand, a positive-negative pneumatic control system is designed (see Fig. 5). The positive and negative pneumatic supply were provided by a mini compressor (USTAR, U-601G) and a vacuum pump (JOANLAB, VP-15S), respectively. Ten compact electro-pneumatic regulators (ITV0030, SMC, Japan) are used to control the ten channels of

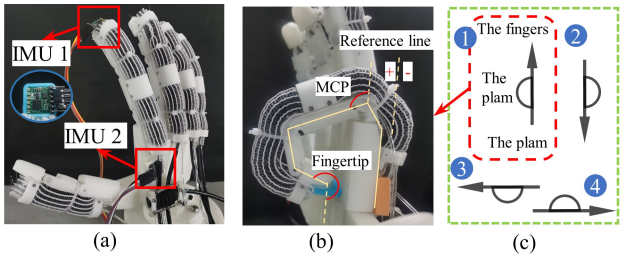

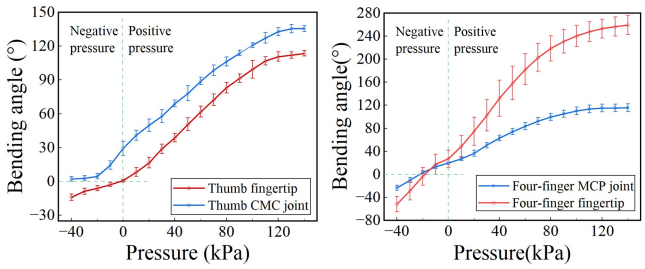

Fig. 7. Bending angle experiment: (a)the experimental set-up, (b)illustration of the fingertip angle and MCP angle, (c)four directions of the hand placement, (d) the results of the thumb as well as (e) the other four fingers.

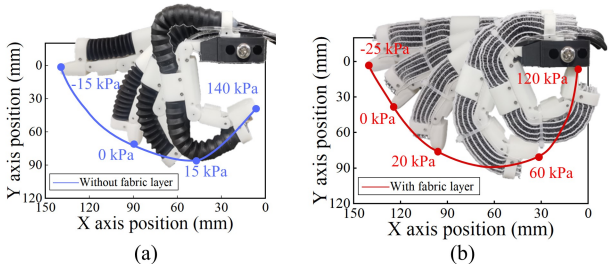

Fig. 8. Finger bending trajectories with (a) and without (b) the fabric layer.

positive air pressure, and one compact electro-pneumatic regulator (ITV0090, SMC, Japan) is used to control the negative air pressure in the inner cavity of the bellows. Ten pulse-triggered switches and ten direct operated poppet type 3-port solenoid valves (VT307V, SMC, Japan) are used to switch the air paths of the positive and negative pressure. Three analogue input and output modules (DAM10AIAO, JY Electronics, China) are used to generate 21 channels of analogue signals, including ten channels for the ITV0030 regulators, one channel for the ITV0090 regulator, and ten channels for the pulse-triggered switches.

III. Experimental Characterization

Characterization experiments were performed including the tests of weight, dimensions, ROM, output force, response time, and stiffness of the hand.

A. Weight and Dimensions

The weight of the robotic hand is 356 g, and the overall length is 205 mm from the tip of the middle finger to the bottom of the palm. Both values are close to the averages for Chinese male adults (380 g and 183 mm).

B. Range of Motion

The motion capacity of a single index finger module is demonstrated in Fig. 6. The bending angles of the five fingers when assembled in the robotic hand were also measured. One inertial measurement unit (IMU) (JY901, Witmotion, China) was attached to the fingertip, and another IMU was placed on

the back of the palm as a reference (see Fig. 7(a)). Before the experiment, the actuator was supplied with a negative pressure to keep the measured finger joint straight, and the two IMU sensors were calibrated. The bending angle was measured relative to the direction of the finger being completely straight, with a positive angle indicating that the finger joint was bent towards the palm (see Fig. 7(b)). Each finger was measured in four directions of the bionic hand placement (as shown in Fig. 7 (c)). Each finger was measured three times in a given orientation, for a total of 12 measurements. The pressure range provided to the actuator was between -40 kPa and 140 kPa with an interval of 10 kPa. As shown in Fig. 7(e), the maximum ROM of the four fingers was from -52° to 259° (with an average repeated accuracy of 3.85°), covering the functional ROM of the human hand. As shown in Table I, we compared the test results with eight other existing dexterous robotic hands. Of the nine hands, this is the only one that achieved a negative bending angle and the ROM is the largest.

Table I
COMPARISON WITH EXISTING DEXTEROUS ROBOTIC HANDS

Reference	Soft-rigid ?	Hand dexterity		Other characteristics (Weight; ROM; Blocking force)
		Kapa-ndji	Feix Grasp	
Our hand	Y	7/10	32/33	356 g; (-52º,259º); 7.5N
Pneumatic [16]	Y	N/A		138 g; (0,130º);0.27 N
Pneumatic [18]	Y	N/A		350 g; (0,275º);15 N
Pneumatic [8]	N	N/A	32/33	300 g; (0,300º); 2.44 N
Pneumatic [12]	N	7/8	31/33	N/A
Motor Tendon[27]	Y	N/A		28 N (All fingers)
FEA&TTA [28]	Y	N/A		1.8 Kg; (0,260º); 4.3 N
Motor [6]	N	8/10	14/14	900 g; 4 N
Motor Tendon [29]	Y	9/10	N/A	300 g; 8N

To verify the effect of the proposed strain limiting layer, tests were conducted to measure the bending trajectories of the index finger with and without the layer. Graph paper was used to record the positions of the vertical projection of the finger under different air pressures. As shown in Fig. 8, the bending angle of the finger without the fabric layer reached 208° under a pressure of 140 kPa, while that with the fabric layer reached 259° under a pressure of 120kPa. The reason for the difference in bending angles could be the energy loss caused by the transverse deformation of the actuators (parallel to the cross section of the finger) occurred when there was no fabric layer.

C. Output Force

Fig. 9(a) and (b) show the settings for measuring the blocking force and bending force of a single finger module. The output force at the fingertip was collected using a 6-axis Force/Torque sensor Nano17 (SI-12-0.12, ATI Nano 17, USA). Data were recorded using a NI acquisition card (NI USB-6210, NI, USA) with a resolution of 0.003 N and a sampling frequency of 1 kHz. The finger was arranged vertically, and a PLA fixture was used to secure the finger and the force sensor. The results are shown in Fig. 9(c). The output bending and blocking force increased roughly linearly with the increase of the input pneumatic pressure, achieving a value of

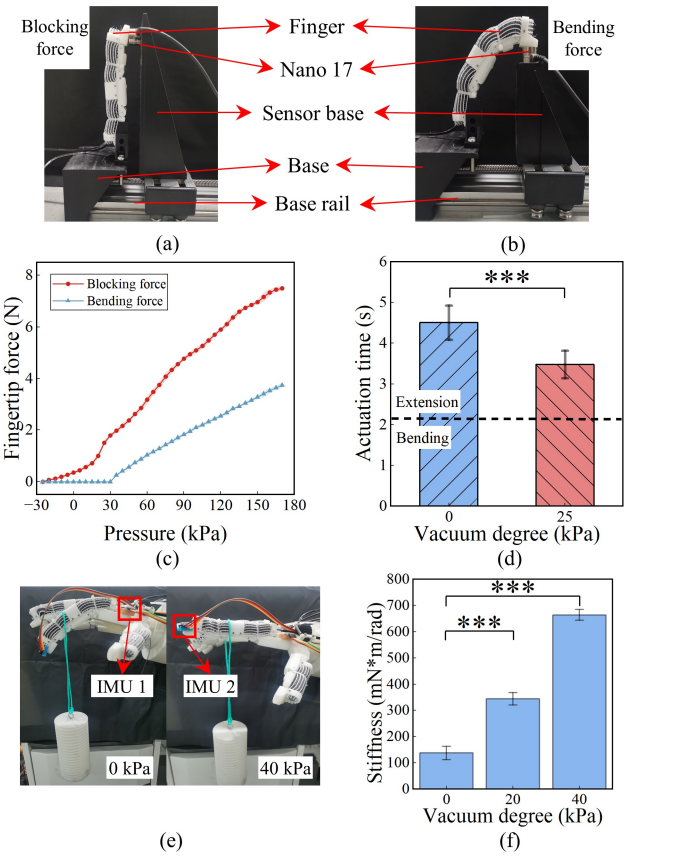

Fig. 9. Experimental set-ups for (a) blocking force measurement and (b) bending force measurement; (c) The bending and blocking forces at the fingertips; (d) The influence of negative pressure on the time required to complete the grasping motion; (e) Weight-bearing performance of the finger at the vacuum pressure of 0 kPa and 40 kPa; (f) The influence of vacuum pressure on the initial stiffness. The symbol *** represents a significant difference between the two groups using student t-test ($p < 0.001$).

3.74 ± 0.09 N and 7.50 ± 0.13 N at a pressure of 170 kPa, respectively. There was a dead zone for the bending force bellow the pressure of 30 kPa. The blocking force achieved here was the third largest compared to the others in Table I.

D. Grasping Motion Speed

Most existing soft robotic hands rely only on the resilience of the material or structure to assist the finger extension motion, increasing the time required to finish the grasping motion [15], [16]. We claim that the proposed robotic hand enables higher motion speed through the proposed bi-directional pneumatic actuation. To validate the statement, we tested the grasping motion time of our robotic hand with and without the proposed negative pressure actuation. The motion process of the robotic hand from the initial state to the maximum bending of all actuators, and then back to the initial state, was defined as one complete grasping motion. In each trial, the robotic hand performed ten complete grasping motions and the time required was recorded. The experiment was repeated five times. As illustrated in Fig. 9(d), upon the addition of negative pressure actuation, the average time required to complete one grasping motion was observed to comprise a full bending motion time of 2.1s and an extension motion time of 1.4s. Notably, the extension motion time of the robotic hand was reduced by approximately 1s, which

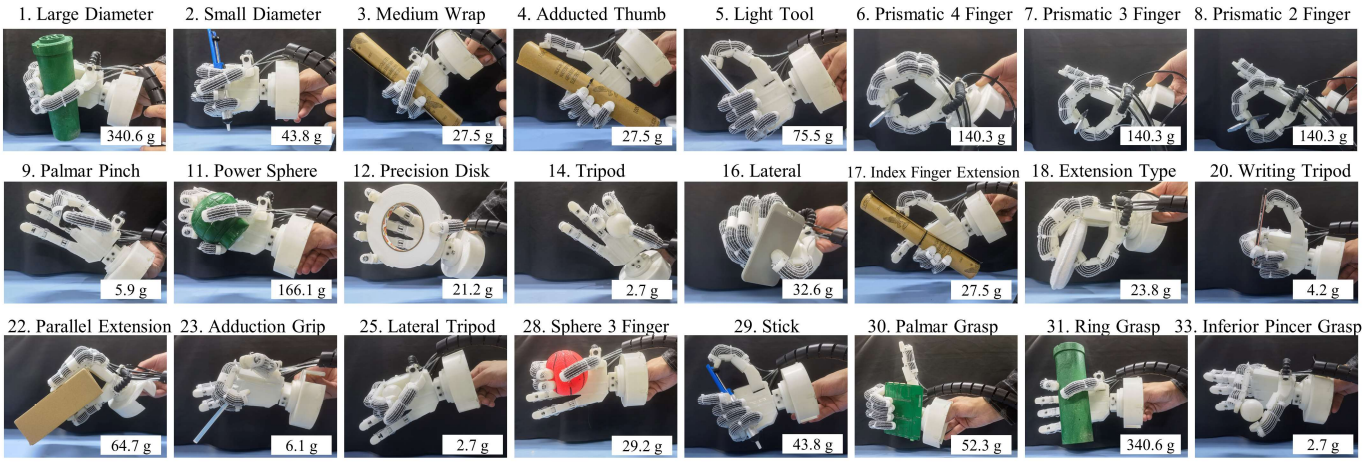

Fig. 10. The results of the grasping performance test: successfully achieved the 24 most frequent grasp types from the Feix taxonomy.

accounts for a reduction of around 42% compared to the extension time without negative pressure.

E. Stiffness

Another advantage of negative pressure in this paper is that the initial stiffness can be increased to stabilize the initial shape of the soft hand, which is conducive to the control of grasp planning and the envelope of the object. The initial stiffness of the robotic finger was also tested with and without our proposed negative pressure actuation. In this experiment, we attached a weight (80 g) to the PIP joint of the index finger and recorded the angular displacement through two IMU sensors (see Fig. 9(e)) under three negative pressure conditions, including 0 kPa, -20 kPa and -40 kPa. As shown in Fig. 9(f), the results demonstrated that providing negative pressure actuation could result in a significant increase in the initial stiffness of the finger.

IV. Grasping Performance

The grasping performance of the hand was evaluated using three tests, including the dexterous grasping test, a thumb dexterity test, and a grasp strength test.

A. Grasping Performance

We used the 24 most frequent grasp types to evaluate the grasping performance of our hands. The Feix taxonomy contains 33 grasping actions, covering most types of grasping in ADLs [30]. Based on the frequency and duration of use, the grasp types with a frequency of less than 0.5% are omitted [30]. The 24 grasp types selected cover 98% of the frequency and 98.6% of the duration of the [31] dataset. A successful grasp was achieved when the hand actively grasps the object and maintains the grasp for at least 5s during movement. As shown in Fig. 10, the anthropomorphic hand could achieve all 24 grasping motions, with three successful consecutive trials. Other grasp types from the Feix taxonomy besides ventral grasp (#32) can also be achieved, although some grasp types have a lower rate of success. The implementation of closed-loop control algorithms utilizing force and position sensors holds the potential to enhance grasping stability. Although, thanks to the design of the palm arch, this hand could rely on the passive clamping force formed between two adjacent fingers when the fingers bent to achieve the adduction grip (#23), there is actually no adduction/abduction actuation of the four fingers in the current hand design.

To validate the design of robotic hands, it is a commonly used way to conduct a dynamic grasping experiment that replicates the three most frequent tabletop grasping strategies in humans, namely, top grasp, flip grasp, and edge grasp [32]. Our robotic hand could successfully replicate all three grasping strategies (see Fig.11(a) - (c)). Notably, the flip grasp had a lower success rate (approximately 50%), which could be attributed to the outline and friction of the fingertip. In addition, the robotic hand could also implement a lateral grasp (see Fig. 11(d)), which is also a commonly used grasping strategy. Before performing the grasping task, the application of negative pressure to induce dorsiflexion motion allows for a wider grasping range of the hand. As shown in Fig. 11 (e) and (f), this allows the hand to easily grasp objects of larger size, such as a square box with a width of 160 mm, a disk with a diameter of 140 mm, and a column with a diameter of 130 mm.

B. Thumb Dexterity

For anthropomorphic hands, the dexterity of the thumb plays a crucial role. The Kapandji finger opposition test is scored by making the tip of the thumb touch 10 different positions [33]. This test was developed to evaluate the movement ability of the thumb before and after surgery or rehabilitation training, and has become one of the most effective ways to test thumb dexterity. The thumb of our robotic hand scored 7 in this test (see Fig. 12), which was the third best compared to the other pneumatic hands in Table I. The thumb was unable to reach the root area of the index and little finger. The reason might be the absence of the rotational DOF in the current thumb design. Hollister et al. [34] argued that the CMC joint of a human thumb contains two non-cross and non-vertical rotation axes. In future work, this rotational DOF can be added to make it more humanoid, and individually actuating the MCP and IP joints of the thumb will also further improve the dexterity.

C. Grasp Strength

As shown in Fig. 13(a), to preliminarily test the grasp strength, lead granules with a diameter of 2 mm (0.05 g per granule) were

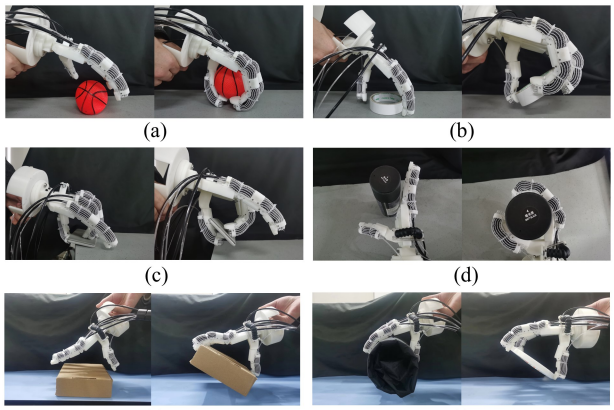

Fig. 11. The proposed hand preforms grasp strategies: (a) top grasp, (b) flip grasp, (c) edge grasp, (d) lateral grasp, (e) and (f) dorsiflexion grasp.

added into a hollow cylinder grasped by the robotic hand until the cylinder slipped off. The results showed that the maximum grasping weight of the hand was 1.86 kg. The friction characteristics of the robotic hand surface and the object surface also affect the test result. To further investigate the grasp strength, we used the standard grasping performance test method proposed by Falco et al [35]. As shown in Fig. 13(b) and (c), a sensor (BSLM-2, BUFSON, China) with a resolution of 0.05N was embedded in a 50mm cylinder. The maximum grasping force was measured under two conditions, namely with the force sensor parallel and vertical to the palm. This experiment was repeated ten times. The results showed that the average maximum grasping force under these two conditions was 17.90 N and 28.15 N, respectively, which are both sufficient to meet the requirements of ADL hand manipulation tasks. In addition, the thin-film pressure sensors (RP-C10-ST-LF, Waaax, China) with an accuracy of 0.05N were used to measure grasp strength of two intermediate and precision grasp type, including palmar pinch and lateral tripod. The sensor was attached to the surfaces of the grasped objects using the two grasps type shown in Fig. 10, and the grasp strength was 5.85N and 13.45N, respectively.

D. Discussion

In this study, a novel anthropomorphic dexterous hand with a soft-rigid hybrid structure and positive-negative pneumatic actuation was proposed. Compared to the robotic hand designed in Zhang et al. [16], our pneumatic soft finger had a significantly larger ROM and output force by using a novel strain limiting method to reduce the energy loss caused by the lateral deformation of the actuator. Compared to the hands proposed in Yan et al. [17] and Liu et al. [18], which both use spring steel straps, our proposed hand achieved more DOFs, higher thumb dexterity, and active bi-directional actuation. It is noteworthy that for pneumatic soft dexterous hands, the advantages brought by positive-negative pressure actuation are significant. This enables the robotic hand to achieve dorsiflexion motion to expand its ROM, and maintaining stiffness before performing the grasping motion will facilitate grasp planning and motion control.

Fiber winding methods are commonly used to make fiber-reinforced bending actuators in soft robotic hands, which have

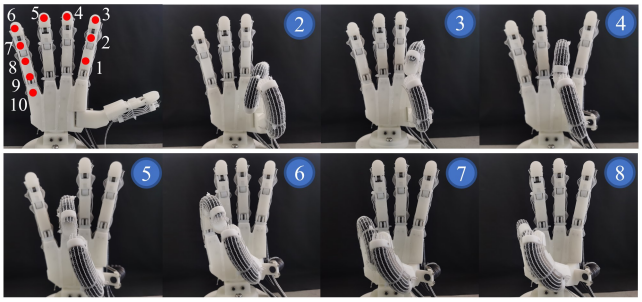

Fig. 12. The proposed hand scored 7 in the Kapandji test.

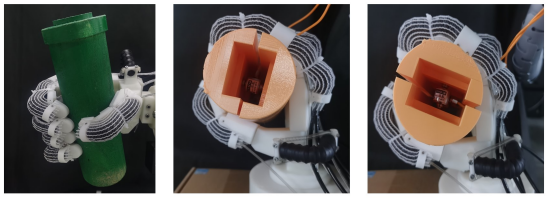

Fig. 13. (a) Grasp strength test for weight holding; Grasping force test with a force sensor (b) parallel and (c) vertical to the palm.

achieved good results in non-functional deformation reduction and increasing output force of pneumatic actuators [12], [13]. In this study, a unidirectional-stretchable nylon elastic fabric was used as a strain limiting layer of the bellows. Both the unidirectional-stretchable nylon elastic fabric and the bellows are off-the-shelf products. The fabrication process was much simpler than fiber winding methods. The experimental results proved that it could also improve the ROM and energy utilization. In future studies, the influence of the parameters of the unidirectional-stretchable nylon elastic fabric on the bending outcomes of the actuators can be further explored. Furthermore, we will select fabric materials with appropriate elongation to replace the tension springs of CMC joint and test the lifespan of the finger. Moreover, while most soft robotic hands, at least for the finger modules, were fabricated in one piece [16], the proposed robotic finger had a modularized design so that damaged parts could be easily replaced.

In the current design, the abduction actuation for the fingers and the rotational DOF, as well as individually actuation of the MCP and IP joints in the thumb have not been realized. In future studies, we can add these missing DOFs, for example, designing multi-DOF for CMC joints to improve thumb dexterity and increasing the motion of metacarpal extension to enlarge the workspace. The weight of the robotic hand is lighter than the average hand weight of a Chinese male hand, while the length is slightly longer than the average length of a Chinese male hand. And the structural shape and size parameters of bellows have a direct impact on the bending performance of bellows [36]. In future work, we aim to further reduce the dimensions of the hand and optimize the parameters of the bellows. And we will design channels to hold the air tube in place to reduce possible motion interference caused by the air tubes.

In this study, the control of the robotic hand was achieved by writing script programs, which was convenient for the grasping performance experiment. For future teleoperation applications, more intuitive control methods, for example using data gloves or EMG sensors, should be introduced.

V. Conclusion

In this research, we developed an anthropomorphic robotic hand with a soft-rigid hybrid structure and positive-negative pneumatic actuation. This robotic hand consisted of five fingers and an arched palm. The fingers in the hand utilize pneumatic actuators composed of soft bellows to actuate a rigid skeleton, forming a soft-rigid hybrid structure with both high adaptability and the ability to provide sufficient stiffness. The positive-negative pneumatic actuation mimics the flexors and extensors of the human hand to implement bi-directional finger actuation. Moreover, different from the commonly used fiber winding method, a unidirectional-stretchable nylon elastic fabric was used as a strain limiting layer of the bellows to increase the ROM and output force of the finger while keeping the assembly process simple. The characteristic experimental results showed that the combined positive-negative pneumatic actuation enlarged the workspace and increased the finger stiffness and speed of motion compared to using only positive pneumatic actuation. The dexterity of this hand was confirmed through grasping performance experiments including Feix taxonomy and Kapandji tests. Compared to other hands in literatures, this robotic hand had good comprehensive performance. Potentially, the robotic hand developed in this study can be used as a substitute for the human hand in tele-operational tasks.

References

[1] G. H. Xu, F. Qi, *et al.*, "Fixed Time Synchronization Control for Bilateral Teleoperation Mobile Manipulator With Nonholonomic Constraint and Time Delay," *IEEE Transactions on Circuits and Systems II: Express Briefs,* vol. 67, no. 12, pp. 3452-3456, 2020.

[2] H. Ding, X. Yang, N. Zheng, M. Li, Y. Lai, and H. Wu, "Tri-Co Robot: a Chinese robotic research initiative for enhanced robot interaction capabilities," *National Science Review,* vol. 5, no. 6, pp. 799-801, 2017.

[3] H. Zhu, X. Li, *et al.*, "Weight Imprinting Classification-Based Force Grasping With a Variable-Stiffness Robotic Gripper," *IEEE Transactions on Automation Science and Engineering,* vol. 19, no. 2, pp. 969-981, 2022.

[4] J. Zhou, X. Chen, U. Chang, J. T. Lu, C. C. Y. Leung, Y. Chen, Y. Hu, and Z. Wang, "A Soft-Robotic Approach to Anthropomorphic Robotic Hand Dexterity," *IEEE Access,* vol. 7, pp. 101483-101495, 2019.

[5] J. Vertongen, *et al.*, "Mechanical Aspects of Robot Hands, Active Hand Orthoses, and Prostheses: A Comparative Review," *IEEE/ASME Transactions on Mechatronics,* vol. 26, no. 2, pp. 955-965, 2021.

[6] D. H. Lee, J. H. Park, S. W. Park, M. H. Baeg, and J. H. Bae, "KITECH-Hand: A Highly Dexterous and Modularized Robotic Hand," *IEEE/ASME Transactions on Mechatronics,* vol. 22, no. 2, pp. 876-887, 2017.

[7] M. Laffranchi, N. Boccardo, *et al.*, "The Hannes hand prosthesis replicates the key biological properties of the human hand," *Science Robotics,* vol. 5, no. 46, pp. eabb0467, 2020.

[8] H. Wang, F. J. Abu-Dakka, *et al.*, "A Novel Soft Robotic Hand Design With Human-Inspired Soft Palm: Achieving a Great Diversity of Grasps," *IEEE Robotics & Automation Magazine,* vol. 28, no. 2, pp. 37-49, 2021.

[9] D. Hidalgo-Carvajal, C. Herneth, A. Naceri, and S. Haddadin, "End-to-End From Human Hand Synergies to Robot Hand Tendon Routing," *IEEE Robotics and Automation Letters,* vol. 7, no. 4, pp. 10057-10064, 2022.

[10] J. Zhou, J. Yi, X. Chen, *et al.*, "BCL-13: A 13-DOF Soft Robotic Hand for Dexterous Grasping and In-Hand Manipulation," *IEEE Robotics and Automation Letters,* vol. 3, no. 4, pp. 3379-3386, 2018.

[11] H. Su, X. Hou, X. Zhang, *et al.*, "Pneumatic Soft Robots: Challenges and Benefits," *Actuators,* vol. 11, no. 3, pp. 92, 2022.

[12] R. Deimel, and O. Brock, "A novel type of compliant and underactuated robotic hand for dexterous grasping," *INTERNATIONAL JOURNAL OF ROBOTICS RESEARCH,* vol. 35, no. 1-3, pp. 161-185, 2016.

[13] P. Polygerinos, *et al.*, "Modeling of Soft Fiber-Reinforced Bending Actuators," *IEEE Transactions on Robotics,* vol. 31, no. 3, pp. 778-789, 2015.

[14] P. Polygerinos, *et al.*, "EMG controlled soft robotic glove for assistance during activities of daily living," *IEEE international conference on rehabilitation robotics (ICORR),* IEEE, 2015.

[15] S. Hashemi, D. Bentivegna, and W. Durfee, "Bone-Inspired Bending Soft Robot," *Soft Robot,* vol. 8, no. 4, pp. 387-396, Aug, 2021.

[16] N. Zhang, L. Ge, H. Xu, X. Zhu, and G. Gu, "3D printed, modularized rigid-flexible integrated soft finger actuators for anthropomorphic hands," *Sensors and Actuators A: Physical,* vol. 312, pp. 112090, 2020.

[17] J. Yan, H. Zheng, F. Sun, H. Liu, Y. Song, and B. Fang, "C-Shaped Bidirectional Stiffness Joint Design For Anthropomorphic Hand," *IEEE Robotics and Automation Letters,* vol. 7, pp. 12371-12378, 2022.

[18] X. Liu, Y. Zhao, D. Geng, S. Chen, X. Tan, and C. Cao, "Soft Humanoid Hands with Large Grasping Force Enabled by Flexible Hybrid Pneumatic Actuators," *Soft Robot,* vol. 8, no. 2, pp. 175-185, Apr, 2021.

[19] Y. Li, Y. Chen, Y. Yang, and Y. Wei, "Passive Particle Jamming and Its Stiffening of Soft Robotic Grippers," *IEEE Transactions on Robotics,* vol. 33, no. 2, pp. 446-455, 2017.

[20] Y. Yang, Y. Zhang, Z. Kan, *et al.*, "Hybrid Jamming for Bioinspired Soft Robotic Fingers," *Soft Robot,* vol. 7, no. 3, pp. 292-308, Jun, 2020.

[21] M. Mentzel, A. Benlic, N. J. Wachter, et al., "The dynamics of motion sequences of the finger joints during fist closure," *Handchir Mikrochir Plast Chir,* vol. 43, no. 3, pp. 147-54, 2011.

[22] M. Suarez-Escobar, and E. Rendon-Velez, "An overview of robotic/mechanical devices for post-stroke thumb rehabilitation," *Disabil Rehabil Assist Technol,* vol. 13, no. 7, pp. 683-703, Oct, 2018.

[23] M. C. Hume, H. Gellman, H. McKellop, and R. H. Brumfield, "Functional range of motion of the joints of the hand," *The Journal of Hand Surgery,* vol. 15, no. 2, pp. 240-243, 1990.

[24] R. Kabir, M. S. H. Sunny, H. U. Ahmed, and M. H. Rahman, "Hand Rehabilitation Devices: A Comprehensive Systematic Review," *Micromachines,* vol. 13, no. 7, pp. 1033, 2022.

[25] K. Matheus, *et al.*, "Benchmarking grasping and manipulation: Properties of the Objects of Daily Living," *IEEE/RSJ International Conference on Intelligent Robots and Systems,* pp. 5020-5027, 2010.

[26] M. Vergara, M. J. Agost, and V. Gracia-Ibáñez, "Dorsal and palmar aspect dimensions of hand anthropometry for designing hand tools and protections," *Human Factors and Ergonomics in Manufacturing & Service Industries,* vol. 28, no. 1, pp. 17-28, 2018.

[27] M. G. Catalano, G. Grioli, *et al.*, "Adaptive synergies for the design and control of the Pisa/IIT SoftHand," *The International Journal of Robotics Research,* vol. 33, no. 5, pp. 768-782, 2014.

[28] Y. Li, Y. Chen, T. Ren, Y. Hu, H. Liu, S. Lin, Y. Yang, Y. Li, and J. Zhou, "A Dual-Mode Actuator for Soft Robotic Hand," *IEEE Robotics and Automation Letters,* vol. 6, no. 2, pp. 1144-1151, 2021.

[29] G. P. Kontoudis, *et al.*, "Open-source, anthropomorphic, underactuated robot hands with a selectively lockable differential mechanism: Towards affordable prostheses." *IEEE/RSJ International Conference on Intelligent Robots and Systems (IROS),* pp. 5857-5862, 2015.

[30] T. Feix, J. Romero, H. B. Schmiedmayer, A. M. Dollar, and D. Kragic, "The GRASP Taxonomy of Human Grasp Types," *IEEE Transactions on Human-Machine Systems,* vol. 46, no. 1, pp. 66-77, 2016.

[31] J. Z. Zheng, *et al.*, "An investigation of grasp type and frequency in daily household and machine shop tasks," *IEEE International Conference on Robotics and Automation,* pp. 4169-4175, IEEE, 2011.

[32] S. Puhlmann, F. Heinemann, *et al.*, "A compact representation of human single-object grasping," *IEEE/RSJ International Conference on Intelligent Robots and Systems (IROS)*, 2016.

[33] A. Kapandji, "Clinical test of apposition and counter-apposition of the thumb," *Annales de Chirurgie de la Main: Organe Officiel des Societes de Chirurgie de la Main,* vol. 5, no. 1, pp. 67-73, 1986.

[34] A. Hollister, W. L. Buford, L. M. Myers, D. J. Giurintano, and A. Novick, "The axes of rotation of the thumb carpometacarpal joint," *Journal of Orthopaedic Research,* vol. 10, no. 3, pp. 454-60, May, 1992.

[35] J. Falco, K. V. Wyk, S. Liu, and S. Carpin, "Grasping the Performance: Facilitating Replicable Performance Measures via Benchmarking and Standardized Methodologies," *IEEE Robotics & Automation Magazine,* vol. 22, no. 4, pp. 125-136, 2015.

[36] C. -H. Liu, L. -J. Chen, J. -C. Chi and J. -Y. Wu, "Topology Optimization Design and Experiment of a Soft Pneumatic Bending Actuator for Grasping Applications," *IEEE Robotics and Automation Letters,* vol. 7, no. 2, pp. 2086-2093, April 2022.